

Land subsidence caused by the East Mesa geothermal field, California, observed using SAR interferometry

Didier Massonnet*, Thomas Holzer †, H el ene Vadon*

*Centre National d'Etudes Spatiales, Toulouse, France

†United States Geological Survey, Menlo Park, USA

Abstract. Interferometric combination of pairs of synthetic aperture radar (SAR) images acquired by the ERS-1 satellite maps the deformation field associated with the activity of the East Mesa geothermal plant, located in southern California. SAR interferometry is applied to this flat area without the need of a digital terrain model. Several combinations are used to ascertain the nature of the phenomenon. Short term interferograms reveal surface phase changes on agricultural fields similar to what had been observed previously with SEASAT radar data. Long term (2 years) interferograms allow the study of land subsidence and improve prior knowledge of the displacement field, and agree with existing, sparse levelling data. This example illustrates the power of the interferometric technique for deriving accurate industrial intelligence as well as its potential for legal action, in cases involving environmental damages.

Introduction

The East Mesa Geothermal Field is located near the east margin of the Salton Sea Trough in the Imperial Valley, southern California, about 25 km east of the town of El Centro. It is one of four geothermal fields, three in the United States and one in Mexico, in this structural depression, that extract geothermal energy. East Mesa generates about 110 MWa of electrical power annually. Although the field was discovered in 1972, significant commercial production did not begin until about 1986 [Signorotti and Hunter, 1992]. Production expanded rapidly until 1989 when it leveled off near current production rates. Today, the 60-km² field annually produces about 90 billion kilograms of water of which 96 percent is reinjected [DOGGR, 1996]. The field is a water-dominated system with primary production between 1829 m and 2280 m. Temperatures of produced fluids range from 146 to 182°C. Fluid is produced from medium-to fine-grained quartzose sandstones [Schatz, 1982].

In this paper, we present the analysis of the site by using interferometric fringes generated by the difference in radar phase acquired at different times by the European ERS-1 satellite in C-band (56 mm wavelength). The images were combined two by two using the digital elevation model elimination method (used here with a "flat" model) which reveals fringes corresponding to contours of equal change in satellite-to-ground distance (i.e., range), which we used previously to sample permanent [Massonnet et al., 1993a; Massonnet et al., 1994; Feigl et al., 1995; Massonnet and

Feigl, 1995a; Murakami et al., 1996] or evolving [Massonnet et al., 1995b; Massonnet et al., 1996] deformation fields with a typical spatial density of ~100 to ~1000 pixels/km². Alternatively, a different implementation of the interferometric technique uses three radar images [Goldstein et al., 1993; Zebker et al., 1994; Peltzer and Rosen, 1995; Peltzer et al., 1996] and does not require the use of an existing topographic model.

Data selection and analysis

The ERS-1 satellite imaged the East Mesa site many times during its second 3-day orbital cycle (sometimes called "winter cycle"). Unlike the first 3-day orbital cycle of ERS-1 (called the "commissioning phase") this orbital cycle was used twice (in 1992 and 1994) and provides the opportunity to work with short term interferograms, separated by a multiple of 3 days during each of the three-month-long cycle, as well as long term interferograms made of radar images separated by roughly two years. The interferometric combinations exhibit various topographic sensitivity, measured by the altitude of ambiguity h_a (the magnitude of unmodelled topography required to create one artifactual fringe [Massonnet and Rabaute, 1993b]). We selected the following ERS-1 data: January 3 and January 27, 1992 as well as February 21 and February 24, 1994. These correspond to image acquisitions from revolutions 2426, 2446, 13614 and 13657, respectively, while the satellite was travelling north to south, with C-band radar looking west at azimuth 281.4° in the "descending" part of the orbit during local daytime (10h 20mn local time) at an angle of incidence of 23.6° from vertical. Taking January 3, 1992, as a reference date, we refer to the images by their dates in days: 0, 24, 780 and 783. Of the six possible pairs, to which we refer by the dates of the participating images and their h_a in meters, we retained four for quantitative analysis, two of the short term kind: (0,24,-58m) and (780,783,-50m), and two of the long term kind: (0,780, 610m) and (24,783, -1040m). Because the terrain is very flat, we did not actually use digital terrain data in the interferometric process, although we have the Digital Terrain Elevation Data (DTED) from USGS for this area. The ground displacement vector projects onto the line of sight, described by the [east, north, up] unit vector from ground to satellite [0.39, -0.08, 0.92] for the center of the East Mesa site, assumed at 32.75N and 115.19W. This vector does not vary significantly over the area of interest. For a geothermal site, we expect only the vertical component to be significant. Each ERS-1 fringe, which corresponds to a change of range of half a wavelength (28 mm), therefore measures a vertical displacement close to 25 mm.

The data were not selected purposely for the detection of surface deformation at the East Mesa geothermal field, but as a general reconnaissance to search for possible impacts from

Copyright 1997 by the American Geophysical Union.

Paper number 97GL00817.
0094-8534/97/97GL-00817\$05.00

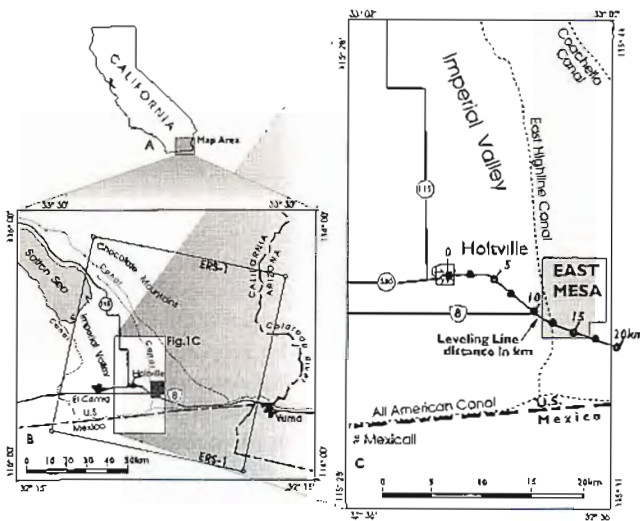


Figure 1. a) General location map of study area; b) location map showing coverage of ERS-1 scenes and area of interferogram used in this study; c) Map of area covered by interferogram shown in figure 2c with (1) administrative boundary of East Mesa geothermal field, (2) location of geodetic leveling profile in figure 3a, (3) East Highline, All American and Coachella canals, and (4) major highways. Most of the area west of the East Highline canal and south of the U.S.-Mexico border, is under cultivation for agriculture. The area is generally flat and lies at an elevation near or below sea level. Geographic coordinates are identical to the ones of a DTED elevation model, not shown here: 1200 points per degree in both latitude and longitude, leading to roughly 92 x 78-m rectangular pixels.

agricultural activities on surface elevations. We were aware that ground water in general in this area is unsuitable for irrigation because of its high salinity. However, we quickly spotted the deformation associated with the geothermal fluid withdrawal at East Mesa, which we knew to be real ground deformation, and not artifact. We also were aware that geothermal energy production can cause subsidence [Narasimhan, 1984]. Deformation caused by mining activity has been documented recently, using radar interferometry [Carnec et al., 1996]. The same technique is used to monitor another geothermal field in Iceland [Vadon and Sigmundson, 1997].

Observations and Modelling

The amplitude part of any of the radar images we used (i.e. the conventional images), show the distinct features indicated on the map (Figure 1). In particular, the Mexican border is outlined by the different ground management used in Mexico (smaller agricultural fields in Figure 2a); the plant itself consists of several bright targets east to the area covered by agriculture; the city of Mexicali, Mexico, appears as a dense collection of bright targets; Interstate I-8 is clearly visible on the image, as is the All American irrigation canal. We apply the pairwise discrimination logic we proposed [Massonnet and Feigl, 1995c] on the six interferograms formed by pair combination of four radar images to exclude any sizable contribution of the atmosphere, the main limiting factor in radar interferometry. This reasoning is valid only on areas which remained coherent in all the interferograms, that is the eastern part of the interferograms and the city of Mexicali. The area covered by agriculture is coherent only on short term

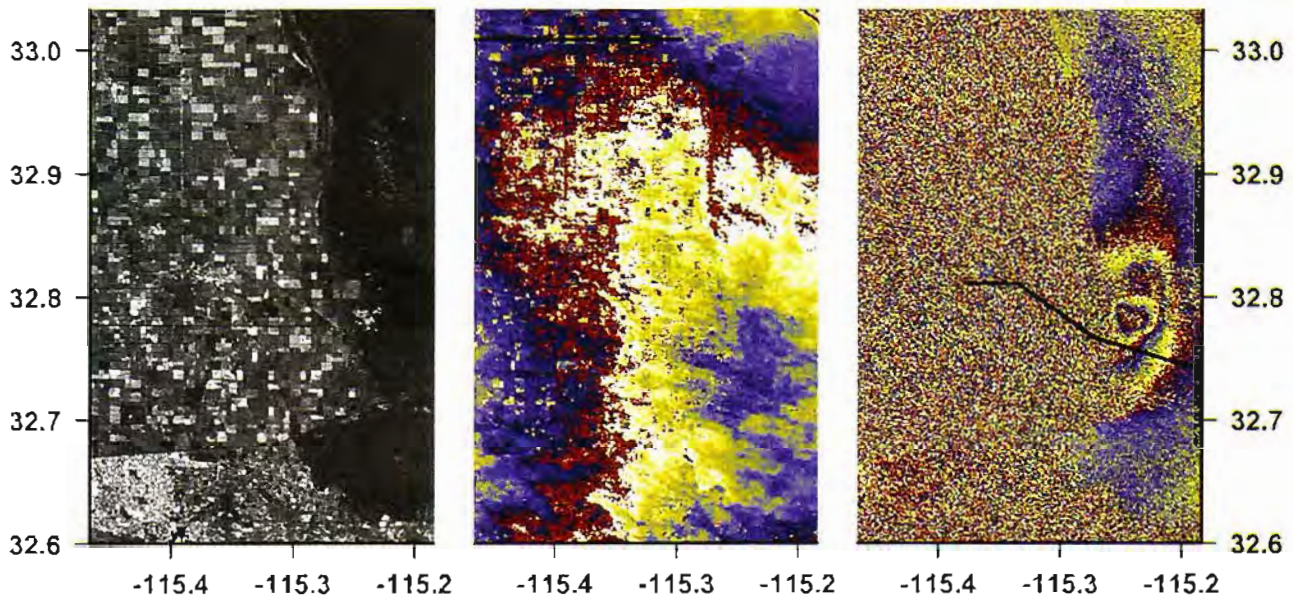


Figure 2. Enlarged portion of the data corresponding to the geometry of map 1c. a) Aspect of the site as the amplitude of a radar image acquired by ERS-1 (orbit 2446 on 3 January 1992), where all the details highlighted in Figure 1c are clearly visible; b) The result of interferometric pair (780, 783, -55m), showing moderate topographic contribution of less than a fringe and surface phase changes on agricultural fields, which remained coherent. The profile used for the estimation of figure 3c is shown; c) The result of interferometric pair (24, 783, -1040m), showing the subsidence caused by the activity of the plant over two years. The fields lost their coherence over the two years elapsed. Topographic residuals cannot mimic more than 1mm of subsidence, since the altitude of ambiguity is some 21 times higher in this pair and the residuals were less than one 28mm fringe in the previous one. From comparison with the remaining interferograms, not shown here, we exclude the subsidence to be an atmospheric artifact, since it appears on the interferogram (0, 780, -50m), made with two independent radar images. Location of leveling profile is shown as 3 dark segments.

interferograms. An obvious explanation of this feature is that the surface is reworked on agricultural fields much more often than every two years, but is not likely to be reworked within three days in February (Figure 2b). On short term interferograms, we observe surface phase changes typical of surfaces having experienced a change in moisture, such as irrigated fields. This phenomenon has been observed for the first time by [Gabriel *et al.*; 1989], using SEASAT data from about the same area. We observe typical changes of 10 mm between adjacent fields (Figure 3b), similar to the ones we documented in the Ukraine [Massonnet and Vadon, 1995d]. On long-term interferograms, the agricultural area has lost its coherence, but an ellipse-shaped area of deformation is clearly visible and centered on the geothermal plant. This deformation is real: it can be seen on all four long term interferograms, excluding any atmospheric propagation change which would be linked to a specific radar image; it can be seen on the interferogram with the lowest sensitivity to topography (about 1000 m for one fringe) whereas the topography cannot create a single fringe at the same location on a short term interferogram much more sensitive to topography (50 m for one fringe). The outer shell of the subsidence area, which correspond to the first 25mm of deformation, is 17km by 8km, or 105km² implying 2.6 million cubic meters of volume loss. The second 25mm is more localized near the southern part of the field, and shows some ragged borders, possibly being more influenced by the positions of the extraction wells. It represents a much lower volume of about 0.8 million cubic meters. Finally, the deformation reaches its highest amplitude of about 75mm in the vicinity of one of the major production areas, representing a small additional volume loss of 0.18 million cubic meters. The total loss of volume is therefore on the order of 3.6 million cubic meters. A direct integration of the volume loss conducted after local "phase unwrapping" of the interferogram gives 3.4 million cubic meters. This figure assumes that the deformation field has east-west symmetry.

Discussion

The radar data are in excellent agreement with leveling data (Fig. 3a) from a first-order leveling line, which passes near the

southern boundary of the field. Both the rates and areal extent of subsidence indicated by relevelings of this line are consistent with the subsidence indicated by the radar interferometry. Maximum rates of subsidence from the 1991-94 relevelings are about 18 mm/yr which compares with 16 mm/yr from 1992-94 interferograms. The accuracy of the result, which we measured by comparing the actual interferogram with a smoothed one, is consistently 0.08 fringes over the areas not used for agriculture, or 2mm rms in terms of subsidence. The radar data, however, provides a more detailed mapping of both the magnitude and areal extend of surface deformation. The proximity of the subsidence area to two canals is of particular concern because canals rely on gravity flow for their operation. Land subsidence from ground water withdrawal has had costly impacts on both the operation and design of canals in California [Prokopovich and Marriott, 1983]. The map indicates that a 13-km-long segment of the East Highline Canal, a north-south canal on the eastern boundary of the agricultural area, is subsiding. The canal passes 2 km west of the point of maximum subsidence. The map also indicates that surface deformation stops about 4.5 km north of the All American canal, which is along the border between the U.S. and Mexico.

The radar interferogram also permits several observations about the relation between geothermal fluid production and subsidence at East Mesa. The interferogram indicates that the maximum subsidence occurs over the southern end of the field, in a small area where about half of the production occurs. In some fields, subsidence is offset from major production areas [Narasimhan, 1984]. The map also permits a direct comparison of the volume of the subsidence bowl to the volume of fluid removed from the geothermal reservoir. Although most of the produced fluid is reinjected, comparison of gross production to reinjected water indicates about 5 million cubic meters of water was removed from the reservoir from 1992 to 1994 [DOGGR, 1995]. This is comparable to the 3.4 million cubic meters volume of the subsidence bowl computed from the interferogram. Both physical compaction and thermal contraction are potential causes of subsidence where geothermal fluids are withdrawn [Narasimhan, 1984]. Unfortunately, pressure and temperature data for fluids produced from East Mesa are proprietary and their

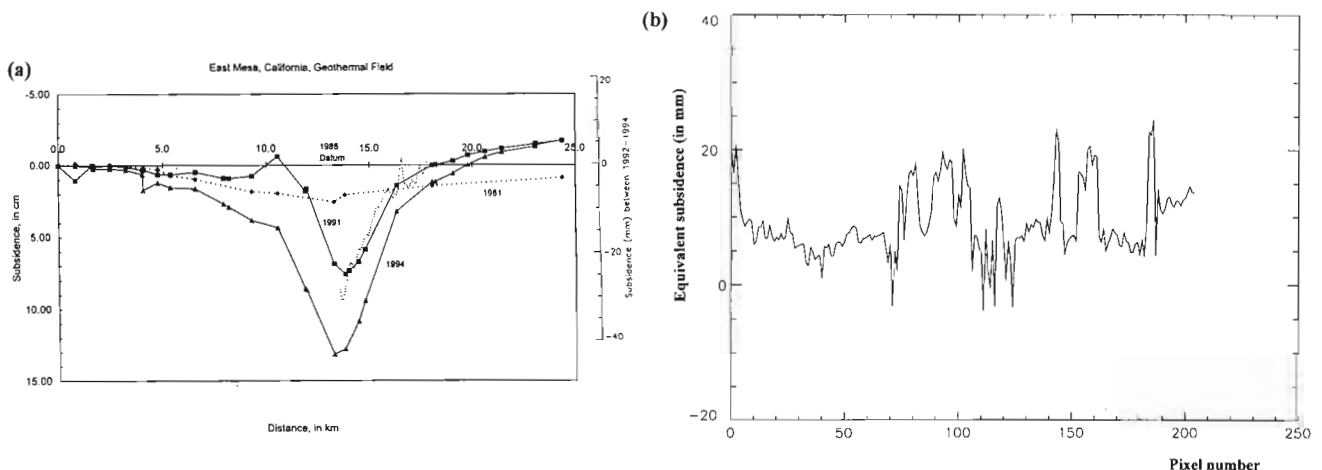


Figure 3. a) Comparison of first-order geodetic leveling data at various dates to a 1988 Datum along the profile of Figures 1c and 2c, together with the interferometric measurement (dotted), wherever it has sufficient clarity. The scale of the interferometric measurement is on the right axis and shows only a two-year subsidence; b) Typical surface phase changes across field on a short term interferogram (Figure 2b), in mm.

unavailability limits speculations about the relative importance of these two mechanisms at East Mesa.

Acknowledgments. We thank Christy Craig Hunter for directing us to information about the East Mesa geothermal field, John Richards for providing geodetic leveling data, and Patrick J. Muffler for sharing his insight into the operation of geothermal fields. We also thank W. Thatcher, M. Murakami as well as an anonymous reviewer for their comments of the manuscript.

References

- Carnec, C., D. Massonnet, and C. King, Two examples of the application of SAR interferometry to sites of small extent, *Geophys. Res. Lett.*, 1996.
- DOGGR, 1995 annual report of the State Oil and Gas Supervisor: California Division of Oil, Gas, and geothermal Resources Publication No. PR06, 279p., 1996.
- Feigl, K. L., A. Sergent, and D. Jacq, Estimation of an earthquake focal mechanism from a satellite radar interferogram: application to the December 4, 1992 Landers aftershock, *Geophys. Res. Lett.*, 22, 9, 1037-1048, 1995.
- Gabriel, A. K., R. M. Goldstein, and H. A. Zebker, Mapping small elevation changes over large areas: differential radar interferometry, *J. Geophys. Res.*, 94, 9183-9191, 1989.
- Goldstein, R. M., H. Engelhardt, B. Kamb, and R. M. Frolich, Satellite radar interferometry for monitoring ice sheet motion: application to an Antarctic ice stream, *Science*, 262, 1525-1530, 1993.
- Massonnet, D., and K. L. Feigl, Discriminating geophysical phenomena in satellite radar interferograms, *Geophys. Res. Lett.*, 22, 1537-1540, 1995a.
- Massonnet, D., and K. L. Feigl, Satellite radar interferometric map of the coseismic deformation field of the M = 6.1 Eureka Valley, California earthquake of May 17, 1993., *Geophys. Res. Lett.*, 22, 12, 1541-1544, 1995b.
- Massonnet, D., P. Briole, and A. Arnaud, Deflation of Mount Etna monitored by spaceborne radar interferometry, *Nature*, 375, 567-570, 1995a.
- Massonnet, D., K. L. Feigl, M. Rossi, and F. Adragna, Radar interferometric mapping of deformation in the year after the Landers earthquake, *Nature*, 369, 227-230, 1994.
- Massonnet, D., and T. Rabaute, Radar interferometry: limits and potential, *IEEE Trans. Geoscience & Rem. Sensing*, 31, 455-464, 1993.
- Massonnet, D., M. Rossi, C. Carmona, F. Adragna, G. Peltzer, K. Feigl, and T. Rabaute, The displacement field of the Landers earthquake mapped by radar interferometry, *Nature*, 364, 138-142, 1993.
- Massonnet, D., W. Thatcher, and H. Vadon, Detection of postseismic fault zone collapse following the Landers earthquake, *Nature*, 382, 612-616, 1996.
- Massonnet, D., and H. Vadon, ERS-1 Internal clock drift measured by interferometry, *IEEE Trans. Geosci. Rem. Sensing*, 33, 2, 401-408, 1995.
- Murakami, M., M. Tobita, T. Saito, and H. Masharu, Coseismic crustal deformations of the 1994 Northridge, California earthquake detected by interferometric analysis of SAR images acquired by the JERS-1 satellite, *J. Geophys. Res.*, 101, 8605-8614, 1996.
- Narasimhan, T.N., Subsidence due to geothermal fluid withdrawal, in Holzer, T.L., ed., *Man-induced land subsidence: Geological Society of America Reviews in Engineering Geology*, VI, 67-105, 1984.
- Peltzer, G., and P. Rosen, Surface displacement of the 17 May 1993 Eureka Valley, California earthquake observed by SAR interferometry, *Science*, 268, 1333-1336, 1995.
- Peltzer, G., P. Rosen, F. Rogez, and K. Hudnut, Postseismic rebound in fault step-overs caused by pore fluid flow, *Science*, 273, 1202-1204, 1996.
- Prokopovich, N.P., and M.J. Marriott, Cost of subsidence to the Central Valley Project, California, *Association of Engineering Geologists Bulletin*, 20, 3, 325-332, 1983.
- Schatz, J.F., Physical processes of subsidence in geothermal reservoirs, *Geothermal Subsidence Research Management Program Report TR 82-39*, 138 p., 1982.
- Signorotti, V., and C.G. Hunter, Imperial Valley's geothermal resource comes of age, *Geothermal Resource Council Bulletin*, 21, 9, 277-288, 1992.
- Vadon, H., and F. Sigmundsson, 1992-1995 Crustal deformation at Mid-Atlantic ridge, SW Iceland, mapped by radar interferometry, *Science*, 275, 193-197, 1997.
- Zebker, H. A., P. A. Rosen, R. M. Goldstein, A. Gabriel, and C. L. Werner, On the derivation of coseismic displacement fields using differential radar interferometry: the Landers earthquake, *J. Geophys. Res.*, 99, 19,617-19,634, 1994.

(Received January 13, 1997; revised March 10, 1997; accepted March 11, 1997.)